

## Ultranarrow lines in Raman spectra of quantum wells due to effective acoustic phonon selection by in-plane wave vector

A. V. Koudinov,<sup>1</sup> E. V. Borisov,<sup>2</sup> A. A. Shimko,<sup>2</sup> Yu. E. Kitaev,<sup>1</sup> C. Trallero-Giner,<sup>3</sup> T. Wojtowicz,<sup>4</sup> G. Karczewski,<sup>5</sup> and S. V. Goupalov<sup>1,6,\*</sup>

<sup>1</sup>*Ioffe Institute, St. Petersburg 194021, Russia*


<sup>2</sup>*Center for Optical and Laser Materials Research, Saint-Petersburg State University, St. Petersburg 198504, Russia*

<sup>3</sup>*Department of Theoretical Physics, Havana University, Havana 10400, Cuba*

<sup>4</sup>*International Research Centre MagTop, Institute of Physics, Polish Academy of Sciences, PL-02668 Warsaw, Poland*

<sup>5</sup>*Institute of Physics, Polish Academy of Sciences, PL-02668 Warsaw, Poland*

<sup>6</sup>*Department of Physics, Jackson State University, Jackson, Mississippi 39217, USA*

 (Received 12 July 2021; revised 24 February 2022; accepted 25 February 2022; published 22 March 2022)

An unusual fine spectrum of very narrow lines ( $<1$  meV overall) is observed in resonance Raman scattering from a CdTe quantum well under normal light incidence, when the laser excitation is about one longitudinal optical (LO) phonon energy higher than the quantum well exciton ground state. The visibility of this fine spectrum is improved by sample doping which reduces the quantum yield of the exciton photoluminescence. The appearance of the four sideway lines of the fine spectrum is explained by the Raman scattering on the combination of LO and longitudinal acoustic (LA) [transverse acoustic (TA)] phonons with the  $e1hh1(2s)$  exciton serving as an intermediate state. The central line is due to elastic scattering of the  $2s$  exciton to the hot  $1s$ -exciton state on a static random potential of the heterostructure followed by emission of a LO phonon.

DOI: [10.1103/PhysRevB.105.L121301](https://doi.org/10.1103/PhysRevB.105.L121301)

Raman scattering in crystals on frequencies different from the frequency of incident light by that of a longitudinal optical (LO) phonon was first observed by Landsberg and Mandelstam in quartz using a mercury light source [1] which required exposition times of 100 h. With the advent of high-power tunable lasers, Raman spectroscopy became far less demanding. Ever since it has been serving as an invaluable source of information about not only the vibrational spectra of solids but also the nature of light-matter interactions. Spectral lines shifted by the combination of frequencies of the LO and longitudinal acoustic (LA) [transverse acoustic (TA)] phonons from the frequency of incident light have been observed in the Raman spectra of bulk semiconductors [2,3] when resonantly excited near the exciton polariton bottleneck region. Together with experiments on Brillouin light scattering [4–7], involving only LA (TA) phonons, these studies have led to the precise experimental determination of exciton polariton dispersion [8,9] in full agreement with theoretical predictions [10,11].

In this Letter we report the observation of Raman scattering on a combination of LO and LA (TA) phonons in semiconductor quantum wells (QWs) at normal incidence. Being quasi-two-dimensional (2D) systems, QW structures cannot support polariton states propagating along the growth axis. Raman spectra from QWs typically consist of sharp optical-phonon lines surrounded by broad and structureless features reflecting the density of states of acoustic phonons [12]. Surprisingly, in the present work we observed characteristic narrow ( $<1$  meV overall) spectra of the scattered light

consisting of five distinct well-resolved lines centered on the frequency of the LO phonon.

Each sample studied in the present work contained three CdTe QWs of different widths [9, 18, and 63 monolayers (MLs), respectively] sandwiched between thick (Cd,Mg)Te barrier layers. Different strengths of the quantum confinement provided independent spectroscopic access to every individual QW. We studied three samples, A, B, and C, which were grown under the same conditions, except that the 18-ML QW of every sample was either undoped (sample A) or doped with rhenium with relatively lower (sample B) or higher (sample C) dopant concentrations. The 18-ML QWs were the main objects of our studies. (See Supplemental Material [13] for details on sample growth.)

All optical spectra in our work were taken at normal light incidence and at temperatures from 2 to 100 K. (See Supplemental Material [13] for details on optical measurements.) Sample characterization revealed a striking effect of rhenium on the photoluminescence (PL) quantum yield. When excited by high-energy quanta in the green spectral range, equally populating excitonic states in all the QWs, PL from the 18-ML QW in sample A was of comparable intensity with that from the 9- and 63-ML QWs [Fig. 1(a)]. In sample B, under the same excitation conditions, emission from the 18-ML QW was dramatically weaker than emission from the remaining two (undoped) QWs [Fig. 1(b)]. In sample C, this effect was even more pronounced. In general, PL from all wide (63-ML) and all narrow (9-ML) QWs, and from the (Cd,Mg)Te barriers did not vary from sample to sample. On the contrary, emission from the 18-ML QW region was very different in intensity for each sample, as selective rhenium doping caused degradation

\*serguei.goupalov@jsums.edu

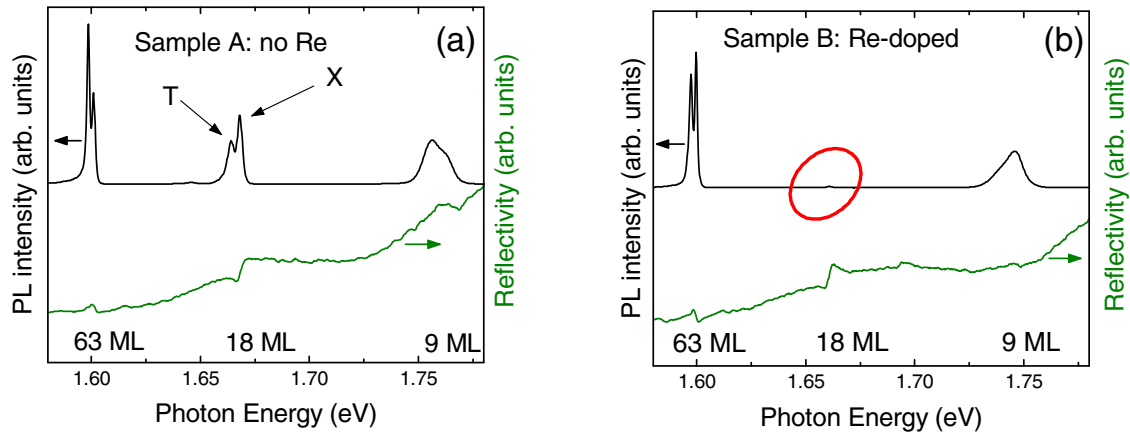


FIG. 1. PL (black line) and reflectivity (green line) spectra of samples A and B, each containing a set of three QWs of different widths (as labeled, in MLs). (a) In the undoped sample A, the 18-ML QW shows a typical PL spectrum consisting of two lines. (b) In sample B subjected to a local rhenium doping, the PL signal from the 18-ML QW is dramatically weaker.

of PL from the doped layers. Quantitatively, the PL intensity from the Re-doped QWs was one to two orders of magnitude weaker as compared to their undoped counterparts.

At the same time, reflectivity spectra did not demonstrate any dramatic change as a result of doping. Well-pronounced excitonic resonance features were present in the spectra of both undoped and doped QWs, as shown in Fig. 1. Moreover, apart from the aforementioned intensity decrease and some additional line broadening (from 3 meV in sample A to 4 meV in sample B to 8 meV in sample C), PL spectra of the 18-ML QWs were not affected by doping. In particular, PL observed from the 18-ML QW in sample B represented a typical, albeit weak, PL spectrum of a high-quality CdTe QW consisting of two lines: the high-energy line assigned to the  $e1hh1(1s)$  exciton resonance [marked as X in Fig. 1(a)] and the low-energy line assigned to the trion resonance [marked as T in Fig. 1(a)]. The intensity ratio of these two peaks usually depends on the experimental conditions. Thus, one can see that doping with rhenium did not cause a catastrophic degradation of the samples' optical quality, but merely introduced centers of nonradiative recombination (“killer centers”) which reduced the PL intensity of rhenium-doped QWs.

The reduced PL background favors observation of the inelastic resonance light scattering mediated by the excitonic states. We will examine the situation when the laser excitation energy exceeds that of the fundamental  $e1hh1(1s)$  excitonic transition by an amount close to the energy of the zone-center LO phonon in CdTe. In Figs. 2(a) and 2(c) we show high-resolution spectra of secondary emission for two slightly different laser energies. In the energy scale of the spectrum shown in Fig. 2(a), the excitonic PL peak, having a full width at half maximum (FWHM) about 4 meV, appears as a wide band exceeding the spectral window of the detector. On that background, one can clearly see a group of well-resolved narrow lines whose approximate linewidths are about 100  $\mu\text{eV}$  (10 CCD pixels). The overall width of this fine spectrum is about 1 meV. The observation of this fine spectrum is our main experimental result.

The fine spectrum exhibits behavior typical for spectra of inelastic light scattering. The energy positions of spectral features follow the laser excitation demonstrating a constant

shift. For sample B, the spectrum consists of five distinct lines. The intensity distribution over the lines forming the fine spectrum stays roughly unchanged when moving over the contour of the exciton PL: The lowest-energy line always remains the most intense. This fine spectrum behaves as a typical resonance process: As the laser energy is fine tuned, the spectrum greatly rises in intensity while sweeping the high-energy wing of the exciton PL peak towards its maximum. As long as the fine spectrum can be resolved, the Raman shifts of its components remain constant and equal 20.52, 20.66, 20.88, 21.10, and 21.23 meV, respectively.

In the stronger-doped sample C, under similar conditions, the fine spectrum is also seen but appears as a group of three resolved lines (of the same net width), as shown in Fig. 3(a). The principle question now arises if the fine spectrum could be observed in the absence of doping. The answer turns out to be affirmative. However, in the undoped sample A, the fine spectrum at resonance is barely visible against the shot noise of the huge PL, as shown in Fig. 3(b). Had we not observed a well-resolved spectral structure in the doped samples, we would probably have overlooked the structure present in the spectrum of sample A.

Let us return to sample B where the fine spectrum is best resolved. We studied the dependence of the emission spectrum on the pump density over two decimal orders of magnitude [one order above and one order below the conditions of Fig. 2(a)]. Both the intensity of the fine spectrum and that of the exciton PL change linearly with the pump intensity. The distribution of lines of the structured spectrum is not sensitive to either pump power or temperature. For temperature and polarization dependences of the spectra, see Supplemental Material [13].

One may suppose that the observed fine spectrum originates from quantization of LO phonons in QWs along the growth direction [16]. However, the appearance of the five-line fine spectrum [Fig. 2(a)] suggests its decomposition into a “central line” (Raman shift 20.88 meV) and two pairs of satellites symmetrically shifted around it akin to Stokes and anti-Stokes components. It turns out that the ratio of the frequency shifts of the outer and inner satellite peaks from the central line is very close to the ratio of the longitudinal and

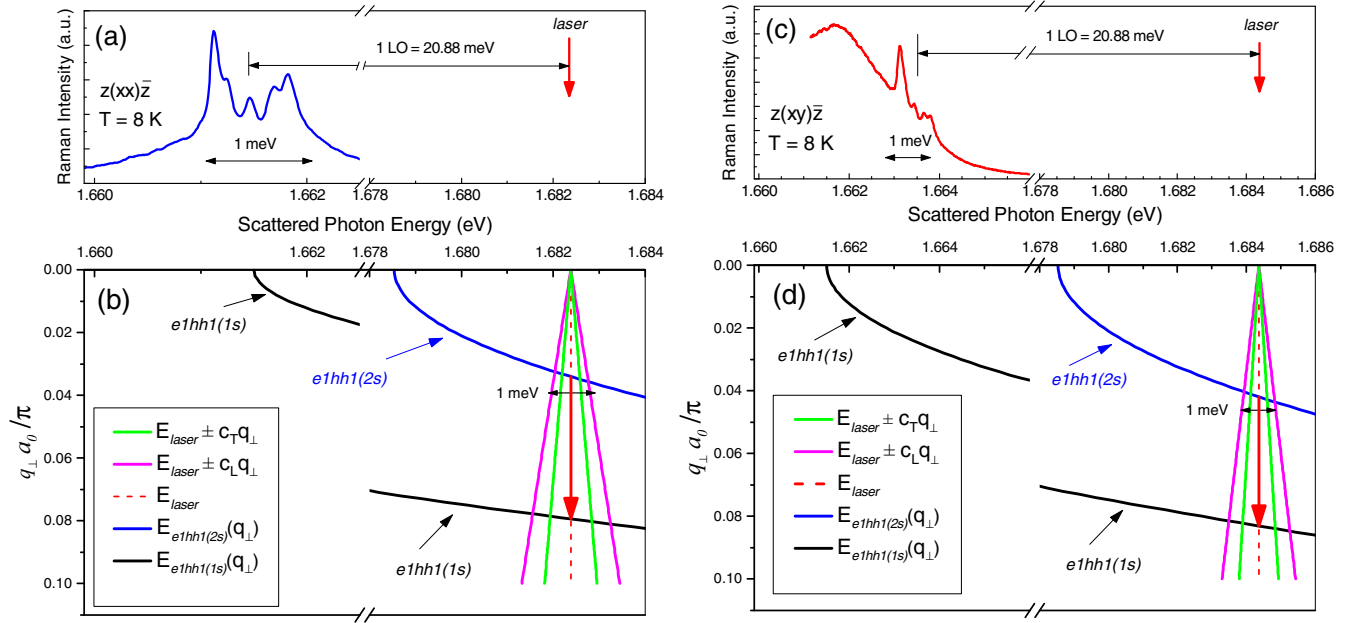


FIG. 2. (a) Emission spectrum from the 18-ML QW in sample B (moderate rhenium doping) under laser excitation (red arrow at 1.682 38 eV) exactly one LO phonon above the  $e1hh1(1s)$  exciton resonance. (b) Calculated energy dispersion curves for  $e1hh1(1s)$  (black line) and  $e1hh1(2s)$  (blue line) excitons as functions of the dimensionless in-plane wave vector  $q_{\perp}a_0/\pi$ . Magenta (green) lines show the dependences  $E_{\text{laser}} \pm c_S q_{\perp}$  with  $S = L(T)$  corresponding to the dispersion of LA (TA) phonons. Intersections of the green and magenta lines with the blue one correspond to the condition of the intermediate resonance leading to the appearance of the side lines on the spectrum in (a). The red arrow indicates elastic scattering of the  $2s$  exciton to the hot  $1s$ -exciton state on a static random potential of the heterointerface responsible for the central line on the spectrum in (a). (c), (d) Same as (a) and (b) but for laser excitation (at 1.684 36 eV) slightly above one LO phonon from the  $e1hh1(1s)$  exciton resonance.

transverse sound velocities in bulk CdTe. This clearly suggests the origin of the outer and inner satellite peaks from the LA and TA phonons and rules out alternate interpretations.

In order to explain the observed fine spectrum we need to invoke not only the exciton ground state,  $e1hh1(1s)$ , but also the higher-lying state of the  $e1hh1(2s)$  exciton. The presence of this state has been detected in CdTe/CdMnTe QWs [17,18] in the PL excitation (PLE) spectra. In order to find its energy position we have performed variational calculations. Since it has been noted [17] that calculated values of the exciton

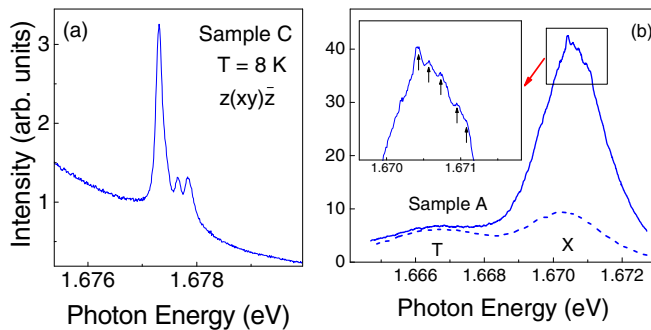


FIG. 3. Fine structures in the emission spectra of the rhenium-doped sample C (a) and in the undoped sample A (b) in the region of the excitonic resonance in the 18-ML QW. Laser excitation at (a) 1.698 48 eV and (b) 1.691 66 eV. The dashed line in (b) represents a “normal” PL spectrum obtained with other (nonresonant) excitation energy. The inset shows a top of the X emission band in the enlarged scale.

binding energies are typically appreciably smaller than the observed values, for our calculations we used the value of the static dielectric constant in the barrier layers  $\epsilon_0 = 9.12$  in order to describe the electron-hole Coulomb attraction in both the barrier and the QW layers (the static dielectric constant of CdTe is 10.4). This gave us the values of the exciton binding energies of 20.45 and 3.41 meV for the  $e1hh1(1s)$  and  $e1hh1(2s)$  excitons, respectively. The resulting order of exciton levels is shown in Figs. 2(b) and 2(d). This figure allows one to understand the origin of the outer (inner) lines of the fine spectrum. The incident light quasiresonantly excites the  $e1hh1(2s)$  exciton. Optical excitation is followed by an emission or absorption of a LA (TA) phonon with a wave vector in the plane of the QW and a transition to the state of the  $e1hh1(2s)$  exciton with the in-plane center-of-mass wave vector  $q_{\perp}$ . Next, emission of an LO phonon accompanies the transition to the state of the  $e1hh1(1s)$  exciton followed by the exciton recombination. The Feynman diagram [19] describing these processes is shown in Fig. 4(a). We note that, since the  $e1hh1(1s)$  and  $e1hh1(2s)$  exciton states are orthogonal, the process involving only the center-zone LO phonon is forbidden.

The energy positions of the inner and outer lines of the fine spectrum are determined by two factors: the condition of the intermediate resonance and the efficiency of the  $e1hh1(2s)$  exciton interaction with LA (TA) phonons. The condition of the intermediate resonance is illustrated in Fig. 2(b) for 2D phonons (having no  $q_z$  component) and incident light on the frequency exceeding the frequency of the  $e1hh1(1s)$  excitonic resonance by that of one LO phonon. The resonant condition

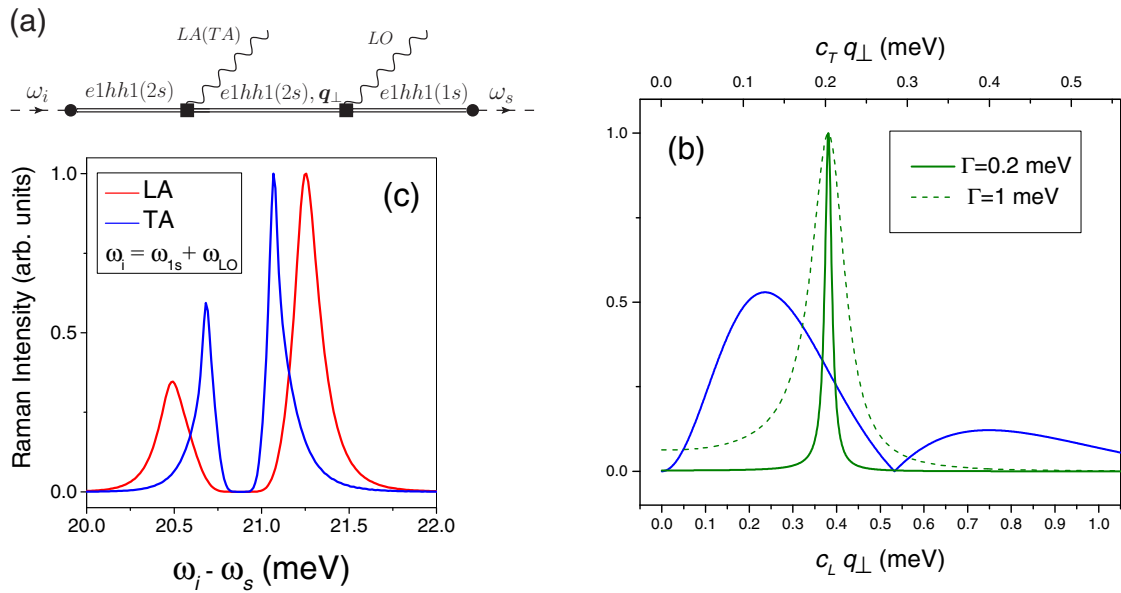


FIG. 4. (a) Feynman diagram [19] corresponding to the scattering process. Incident light excites the  $e1hh1(2s)$  exciton which gets scattered to the state of the  $e1hh1(2s)$  exciton with a finite in-plane center-of-mass wave vector by emission (absorption) of the acoustic phonon. The subsequent transition to the  $e1hh1(1s)$  exciton state is assisted by emission of the LO phonon. The scattered light is emitted after recombination of the  $e1hh1(1s)$  exciton. (b) Relative contributions of the exciton-phonon coupling (blue solid line) and intermediate resonance profile with exciton decay rates of  $\Gamma = 0.2$  meV (green solid line) and  $\Gamma = 1$  meV (green dashed line) to the spectral line as a function of LA-phonon energy (lower scale) and TA-phonon energy (upper scale). (c) Calculated normalized spectra corresponding to the scattering process with the participation of the LA (red line) and TA (blue line) phonon at  $T = 8$  K. Excitation energy is the same as in Fig. 2(a).

is satisfied when the green and magenta lines intersect in Fig. 2(b) with the blue line, describing the dispersion of the  $e1hh1(2s)$  exciton. The relative roles of the two factors are illustrated in Fig. 4(b). When the exciton decay rate is relatively low, then the energy denominator in the expression for the scattering rate (see Supplemental Material [13]) corresponding to the intermediate resonance leads to a sharp resonance profile which mainly determines the energy positions of the satellite lines in Raman spectra. For higher exciton decay rates this resonance profile is wider and the positions of the satellite lines are determined by both resonance conditions and the energy dependence of the exciton-phonon coupling. In the latter case the positions of the satellite lines are less sensitive to the change of resonance condition induced by the change of the excitation energy. We believe that this case describes our experimental observations. The interplay of these two factors leads to an effective selection of acoustic phonons by the in-plane wave vector which determines the energy positions and linewidths of the satellite lines.

We calculated normalized spectra corresponding to the light scattering on the combination of LO and LA (TA) phonons. In this calculation we used the values of sound velocities of  $c_L = 3.35 \times 10^5$  cm/s ( $c_T = 1.79 \times 10^5$  cm/s) for the longitudinal (transverse) sound in CdTe, averaged over the sound propagation directions. These calculations also allow for finite components of the phonon wave vectors along the growth direction. The outcomes of our calculations are shown in Fig. 4(c). The excitation energy was chosen to coincide with the excitation energy in the experimental spectrum shown in Fig. 2(a). One can see that the results of the calculation closely reproduce the energy positions of the outer and inner lines of the experimentally observed fine spectra. For these model

calculations, we took the widths of all the exciton resonances (incoming, intermediate, and outgoing) to be equal to 1 meV (see Supplemental Material [13] for more calculated spectra).

Now we should discuss the origin of the central line in the fine spectrum [cf. Fig. 2(a)]. In Ref. [18] a double resonance in secondary emission has been studied in a semimagnetic CdTe/Cd<sub>1-x</sub>Mn<sub>x</sub>Te multiple QW structure at  $T = 1.6$  K. The double resonance was achieved by a resonant laser excitation of the  $e1hh1(2s)$  exciton and optical detection resonant with the energy of the  $e1hh1(1s)$  exciton. A strong diamagnetic shift of the  $2s$  exciton in an external magnetic field allowed one to tune the  $2s$ - $1s$  spacing in the range from 16.2 meV at zero field to 25 meV at  $B = 9.4$  T in an 85-Å-wide QW [18]. When this spacing was in resonance with the energy of a LO phonon ( $\sim 21$  meV), a strong enhancement in the intensity of the detected signal was observed. Depending on polarization, such an enhancement was observed for two different magnetic fields corresponding to the resonances between different Zeeman-split exciton sublevels. This behavior was explained by the elastic scattering of the  $2s$  exciton to the state  $|e1hh1(1s), q_{\perp}\rangle$  of the  $1s$  exciton with a large in-plane center-of-mass wave vector  $q_{\perp}$  with subsequent multiple scattering by a static random potential of the heterostructure and emission of a LO phonon [see the red arrow in Fig. 2(b)]. Similar explanations were suggested for observations of double resonances in secondary emission in the bulk materials [20] and in GaAs/Al<sub>x</sub>Ga<sub>1-x</sub>As QWs [21]. We believe that a similar mechanism underlies the appearance of the central peak in our spectra.

To conclude, we have observed the fine structure of spectral lines in Raman scattering from QWs under normal incidence. The lines shifted from the LO-phonon line by 2–3  $\text{cm}^{-1}$  were

resolved. The outer (inner) lines in the observed spectrum are explained as originating from the Raman scattering on the combination of LO and LA (TA) phonons with the  $e1hh1(2s)$  exciton as an intermediate state. The central line is due to elastic scattering of the  $2s$  exciton to the hot  $1s$ -exciton state on a static random potential of the heterostructure, followed by emission of a LO phonon. The observed phenomenon is masked by the strong PL but has a universal character and can be enhanced in doped samples, where PL is suppressed.

We would like to thank A. N. Reznitsky, A. V. Sel'kin, V. F. Sapega, B. H. Bairamov, V. A. Kosobukin, and E. L. Ivchenko for useful discussions. Theoretical calculations were done by S.V.G. and supported by the Russian Science Foundation Grant No. 20-42-04404. The work was partially supported by RFBR Grant No. 19-02-00422. The research in Poland was partially supported by the Foundation for Polish Science through the IRA Programme cofinanced by EU within SG OP (Grant No. MAB/2017/1) and by the National Science Centre through Grant No. 2018/30/M/ST3/00276.

- 
- [1] G. S. Landsberg and L. I. Mandelstam, A new phenomenon in scattering of light in crystals (in German), *Naturwiss.* **16**, 557 (1928).
- [2] E. S. Koteles and G. Winterling, Resonant scattering of exciton polaritons by LO and acoustic phonons, *Phys. Rev. B* **20**, 628 (1979).
- [3] Y. Oka and M. Cardona, Resonance Raman scattering of excitonic polaritons by LO and acoustic phonons in ZnTe, *Solid State Commun.* **30**, 447 (1979).
- [4] R. G. Ulbrich and C. Weisbuch, Resonant Brillouin Scattering of Excitonic Polaritons in Gallium Arsenide, *Phys. Rev. Lett.* **38**, 865 (1977).
- [5] G. Winterling and E. S. Koteles, Resonant Brillouin scattering near the A-exciton in CdS, *Solid State Commun.* **23**, 95 (1977).
- [6] G. Winterling, E. S. Koteles, and M. Cardona, Observation of Forbidden Brillouin Scattering near an Exciton Resonance, *Phys. Rev. Lett.* **39**, 1286 (1977).
- [7] P. Y. Yu and F. Evangelisti, Two-phonon resonant Brillouin scattering in CdS, *Solid State Commun.* **27**, 87 (1978).
- [8] E. S. Koteles, Investigation of exciton-polariton dispersion using laser techniques, in *Excitons*, edited by E. I. Rashba and M. D. Sturge (North-Holland, Amsterdam, 1982), p. 85.
- [9] C. Weisbuch and R. G. Ulbrich, Resonant light scattering mediated by excitonic polaritons in semiconductors, in *Light Scattering in Solids III*, edited by M. Cardona and G. Güntherodt (Springer, Berlin, 1982), Chap. 7.
- [10] J. J. Hopfield, Theory of the Contribution of Excitons to the Complex Dielectric Constant of Crystals, *Phys. Rev.* **112**, 1555 (1958).
- [11] W. Brenig, R. Zeyher, and J. L. Birman, Spatial dispersion effects in resonant polariton scattering. II. Resonant Brillouin scattering, *Phys. Rev. B* **6**, 4617 (1972).
- [12] P. S. Kop'ev, D. N. Mirlin, V. F. Sapega, and A. A. Sirenko, Geminant radiative recombination in GaAs/AlGaAs quantum-well structures in magnetic field, *JETP Lett.* **51**, 708 (1990) [*Pis'ma Zh. Eksp. Teor. Fiz.* **51**, 624 (1990)].
- [13] See Supplemental Material at <http://link.aps.org/supplemental/10.1103/PhysRevB.105.L121301> for details of the experiment and calculations, which includes Refs. [14,15].
- [14] P. Venzuela, M. Lazzeri, and F. Mauri, Theory of double-resonant Raman spectra in graphene: Intensity and line shape of defect-induced and two-phonon bands, *Phys. Rev. B* **84**, 035433 (2011).
- [15] V. N. Popov, Two-phonon Raman bands of single-walled carbon nanotubes: A case study, *Phys. Rev. B* **98**, 085413 (2018).
- [16] A. Bruchhausen, A. Fainstein, B. Jusserand, and R. André, Resonant Raman scattering by CdTe quantum-well-confined optical phonons in a semiconductor microcavity, *Phys. Rev. B* **73**, 085305 (2006).
- [17] S. R. Jackson, J. E. Nicholls, W. E. Hagston, P. Harrison, T. Stirner, J. H. C. Hogg, B. Lunn, and D. E. Ashenford, Magneto-optical study of excitonic binding energies, band offsets, and the role of interface potentials in CdTe/Cd<sub>1-x</sub>Mn<sub>x</sub>Te multiple quantum wells, *Phys. Rev. B* **50**, 5392 (1994).
- [18] D. R. Yakovlev, W. Ossau, A. Waag, G. Landwehr, and E. L. Ivchenko, Double  $2s$ - $1s$  resonance in LO-phonon-assisted secondary emission of quantum-well structures, *Phys. Rev. B* **52**, 5773 (1995).
- [19] P. Y. Yu and M. Cardona, *Fundamentals of Semiconductors. Physics and Materials Properties*, 4th ed. (Springer, Heidelberg, 2010).
- [20] S. I. Gubarev, T. Ruf, and M. Cardona, Doubly resonant Raman scattering in the semimagnetic semiconductor Cd<sub>0.95</sub>Mn<sub>0.05</sub>Te, *Phys. Rev. B* **43**, 1551 (1991).
- [21] D. A. Kleinman, R. C. Miller, and A. C. Gossard, Doubly resonant LO-phonon Raman scattering observed with GaAs/Al<sub>x</sub>Ga<sub>1-x</sub>As quantum wells, *Phys. Rev. B* **35**, 664 (1987).